Modelling of the SCC crack growth for low alloy steels in high temperature water

B. Tirbonod
Laboratory for Safety and Accident Research
Paul Scherrer Institute
CH-5232 Villigen PSI (Switzerland)

Abstract

For the crack growth mechanism of low alloy steels in oxygenated high temperature water, an anodic dissolution generated by the rupture of the oxide film at the crack front, followed by a repassivation and by a cleavage, is assumed. The model presented here is the contribution of the anodic dissolution to the crack growth. It uses well accepted laws of electrochemistry with parameters scanning their known spectrum of values and the assumption of homogeneity for the electrolyte. An important result is the dimension of the dissolution cell of the order of the micrometer. For a same value of the conductivity, the results strongly differ according to the ions predominant in the electrolyte (SO^4_{2-} and Fe^{2+} ions for the effects of the repassivation and of the equilibrium potentials, respectively).

Keywords: stress corrosion cracking, low alloy steels, anodic dissolution, repassivation.

Introduction

A model for the Stress Corrosion Cracking of Low Alloy Steels under Boiling Water Reactor conditions is in course of development at the Paul Scherrer Institut [1a,1b]. The crack growth mechanism assumed for these steels, based on that considered in other models [2,3] and observations [4,5a], includes the following sequence: rupture of the protective oxide film at the crack front, crack advance by anodic dissolution of the bare metal and by cleavage, and repassivation at the crack front. The model presented here is the part dealing with the contribution of the anodic dissolution to the crack growth. It considers physically the parameters expected to be of relevance at the crack front (composition of the electrolyte, conductivity, cell dimensions, exchange current densities, oxide film rupture frequency). The paper presents the model, a parametric sensitivity study with highlight to the repassivation and to maximum cases for the crack advance, and a discussion.

Model

The crack, assumed to be present in a pure iron specimen, is loaded to a stress intensity factor K_I. The dissolution cell is three dimensional with the anode situated at the crack tip and the two cathodes on the crack flanks (Fig.1). The height of the cell (H_0 in Fig. 1) is assumed to be the Crack Tip Opening Displacement (CTOD). The rupture of the oxide film is assumed to be generated by dislocations emerging by creep at the crack tip. The CTOD is calculated together with the creep rate for a given K_I by using a viscoplastic model and the finite elements [6]. The electrodes are assumed to be homogeneous. The cross section of the growing dissolution cavity is the

anode surface. The electrolyte, assumed to be dilute, electroneutral, chemically neutral ($pH_{25^\circ C}$ = 7), and homogeneous, is composed of water with the ions Fe^{2+}, NO_3^-, H^+, OH^-, Na^+, and SO_4^{2-}, resulting from the dissociation of $Fe(NO_3)_2$, H_2O and Na_2SO_4, respectively.

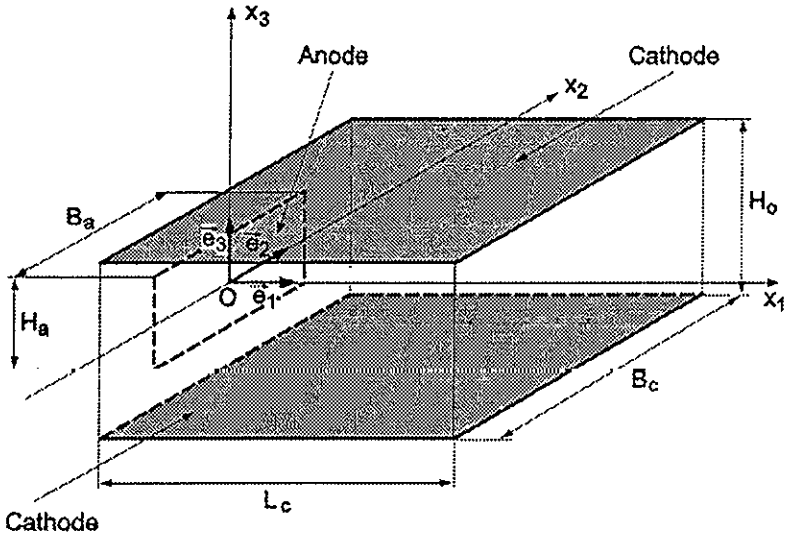

Figure 1: Scheme of the dissolution cell. The anode is assumed to be situated at the crack tip and the two cathodes on the crack flanks.

The anodic and cathodic reactions will be the oxidation of iron and the reduction of H^+, respectively. The Fe^{2+} and H^+ concentrations provide the anodic and cathodic equilibrium potentials of these reactions, respectively, calculated with the Nernst law. The equations for the anodic and cathodic currents and for the anodic and cathodic potentials include the Butler-Volmer law, the charge conservation principle, and the Ohm law. The dissolution propagation length per dissolution event (a_d) is calculated from the anodic current density with the Faraday law; the repassivation is considered by a time law in $(t/t_0)^{-p}$, where t is the time and t_0 and p the oxide film nucleation time and an exponent, respectively, both depending on the SO_4^{2-} concentration (Fig. 2, referred in [5b]). The resistance of the cell is calculated by assuming straight current lines. The equations as well as the

values of the parameters, which scan their whole range of values known from the literature, are given in [1a,1b].

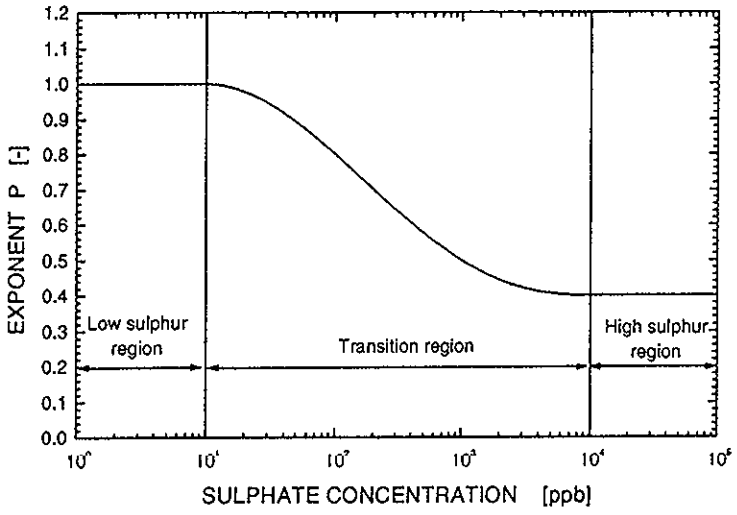

Figure 2. Exponent p as a function of the SO_4^{2-} concentration.

Results

The two types of electrolytes considered, characterized by predominant increasing concentrations at the crack tip in either Na^+ and SO_4^{2-} or Fe^{2+} and NO_3^- ions exhibit the same conductivity (between 0.08 and 63 µS/cm at 25°C), but very different behaviours for a_d (Fig.3). The critical effect of the repassivation due to the SO_4^{2-} ions clearly appears by comparing to the results obtained for predominant Fe^{2+} and NO_3^- ions (the difference on a_d can amount up to a factor 800), a result in agreement with the literature [7]. For the latter case, the decreasing phases are due to the increasing value of the equilibrium anodic potential at increasing Fe^{2+} concentrations and at constant equilibrium cathodic potential, with a strong dependence on the values of the anodic and cathodic exchange current densities (i_{a0} and i_{c0}, respectively). The model clearly makes to appear that the significant

parameter for the anodic dissolution is not the conductivity but the composition of the electrolyte which affects the repassivation (SO_4^{2-}) or the equilibrium potentials (Fe^{2+}).

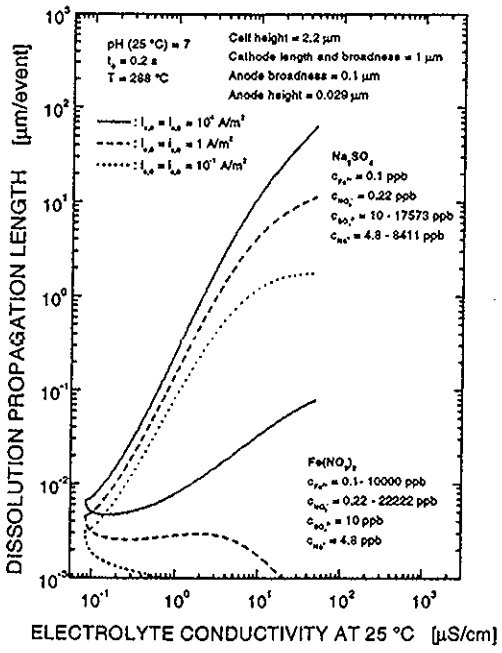

Figure 3: Dissolution propagation length per dissolution event as a function of the electrolyte conductivity at 25°C for two electrolytes dominant in either Fe^{2+} and NO_3^- ions or Na^+ and SO_4^{2-} ions and for different values of the anodic and cathodic exchange current densities assumed to be equal (10^4, 1 and 10^{-1} A/m^2).

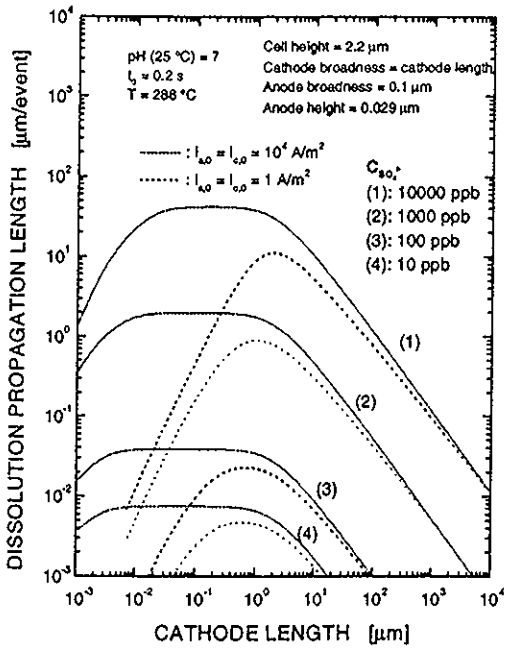

Figure 4: Dissolution propagation length per dissolution event as a function of the cathode length and broadness for different values of the SO_4^{2-} concentration and of the anodic and cathodic exchange current densities assumed to be equal (10^4 and 1 A/m^2).

Figure 4 shows that a_d increases with the cathode length and broadness (scanned range: 0.001 - 10000 µm) to reach a maximum or a plateau in the range about 0.005 - 2 µm, depending on the values of the exchange current densities, and then decreases at higher values. This is true for all values of the SO_4^{2-} concentration. The increasing phase is attributed to the increasing cathode to anode area ratio and the decreasing phase to the increase of the electrolyte resistance due to increasing dimensions of the cell. This result confirms that the active part of the dissolution cell is situated in the very vicinity of the crack tip, as certain authors have proposed on the basis of experiments [7]. This does not support the assumption of the external surface of the crack for the cathode made in [3]. There is no significant dependence on the anode dimensions [1b]. One can define a characteristic length of the order of the micrometer for the dissolution cell.

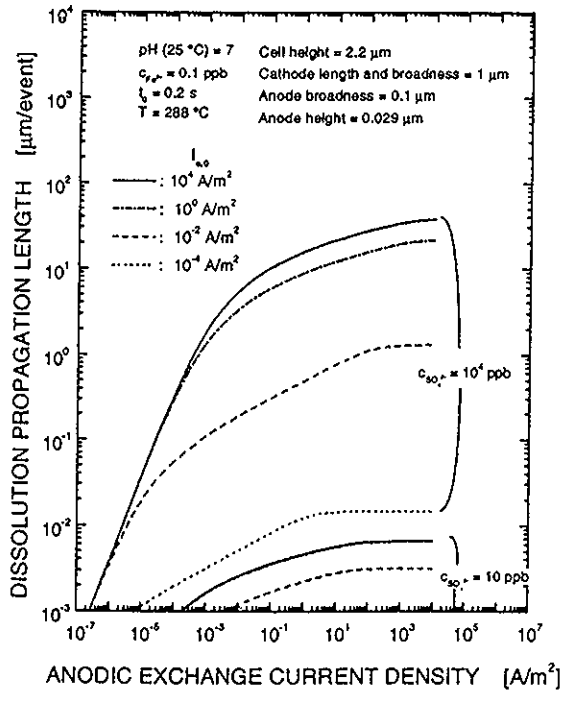

Figure 5: Dissolution propagation length per dissolution event as a function of the anodic exchange current density for different values of the cathodic exchange current density (10^4, 1, 10^{-2} and 10^{-4} A/m^2) and of the SO_4^{2-} concentration (10^4 and 10 ppb).

The sensitivity of a_d to the anodic exchange current density strongly depends on the cathodic exchange current density and on the SO_4^{2-} concentration (Fig. 5).

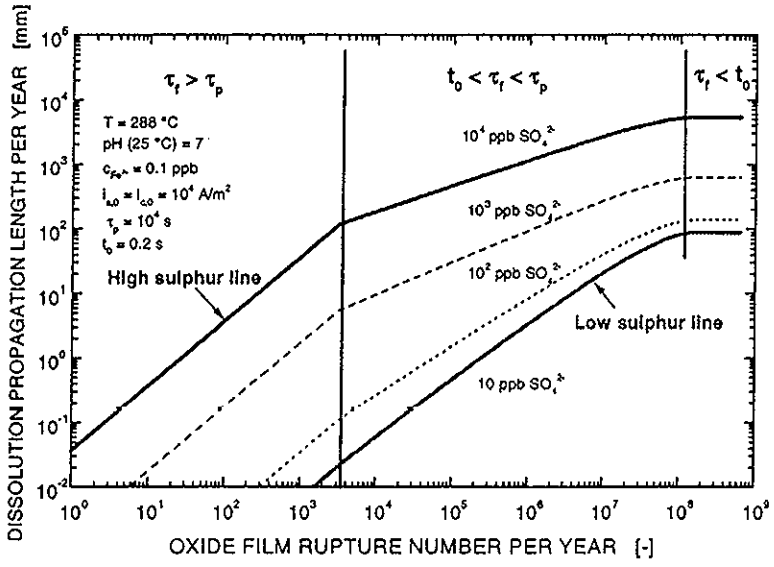

Figure 6: Dissolution propagation length per year as a function of the oxide film rupture number per year for different SO_4^{2-} concentrations.

The dissolution propagation length per year is the product of a_d with the oxide film rupture number per year (which determines the time interval between two oxide film ruptures τ_f). It exhibits (Fig. 6) as a function of the oxide film rupture number per year three regions for a given value of the SO_4^{2-} concentration according to the values of τ_f with respect to that of the repassivation time τ_p . In the first region ($\tau_f > \tau_p$), a_d increases with about the same rate at any SO_4^{2-} concentration: the effect of the repassivation is very small and the relevant parameter is the conductivity. In the second region ($t_0 < \tau_f < \tau_p$), a_d still increases but with a rate depending on τ_f (the dissolution time decreases by decreasing τ_f) and on the SO_4^{2-} concentration in connection to the repassivation. In the third region ($\tau_f < t_0$), a_d remains

constant: there is no more repassivation (the dissolution is continuous) and a_d depends only on the conductivity. These results show the presence of the so-called low and high sulphur lines found by experiments (referred in [5a]), for the oxide film rupture number per year here.

Discussion

The main limitations of the model include the non-consideration of the concentration gradients in the electrolyte and the material embedding the crack (assumed to be pure iron), in connection to the electrolyte composition and electrochemical reactions. For the first case, the Butler-Volmer law, which connects the current density to the overpotential at an electrode, gives the maximum value for the current density which is limited by only the polarization resistance of the electrode. Thereby, the presence of diffusion gradients in the electrolyte as well as the resistance of the electrolyte will make to decrease the current density. Therefore, neglecting the concentration gradients is conservative for the calculation of a_d. The second case mainly deals with the presence in the low alloy steels of precipitates among which manganese sulphide (MnS) inclusions whose dissolution results in the presence of sulphur ions and compounds in the electrolyte with the corresponding delay for the repassivation. The dissolution of the precipitates can be included in the model by considering the corresponding ions and electrochemical reactions; for the MnS inclusions, the dissolution is implicitly included in the SO_4^{2-} concentration assumed for the electrolyte in the cell.

Further application of the model for crack growth calculations requires estimating the values of the sensitive parameters which were found to be the

electrolyte composition at the crack tip and the exchange current densities (their values cannot be predicted [8]), and of the cleavage length. Work is in progress for estimating these parameters from experiments [4] with the present model in connection to a viscoplastic model [1b,6]. Additional information on the electrolyte composition at the crack tip, which depends on the composition outside the crack by the species transport along the crack, is expected from solving the transport equation considered with the charge conservation [1b].

Conclusions

A characteristic length for the dissolution cell, of the order of the micrometer, has been put in evidence. This result supports the assumption that the dissolution cell resulting in the crack growth is situated in the very vicinity of the crack tip.

The model is in agreement with the existence of the so-called low and high sulphur lines for the dissolution propagation length found by experiments. The relevant parameters are the composition of the electrolyte, not the conductivity, by effects related to the repassivation and to the equilibrium potentials, as well as the exchange current densities and the oxide film rupture frequency.

Acknowledgements

This work has been financially supported by the Swiss Federal Office of Energy (BEF) and by the Swiss Federal Nuclear Safety Inspectorate (HSK).

Literature References

[1] B. Tirbonod, (a) Proposed Models for the Stress Corrosion Cracking, PSI internal report TM-49-97-01 (1997), (b) to be published

[2] F. P. Ford, Slip Dissolution Model, Corrosion sous Contraitne, Phénoménolgie et Mécanismes, D. Desjardins et R. Oltra eds, Les Editions de Phyique, Les Ulis (F), (1992),307,344

[3] D.D. Macdonald and M. Urquidi-Macdonald, A Coupled Environment Model for Stress Corrosion Cracking in Sensitized Type 304 Stainless Steel in LWR Environment, Corr. Sci. 32 (1991), 51,81

[4] H.P. Seifert, J. Heldt and U. Ineichen, to be published

[5] V. Läpple, Untersuchungen zum Korrosiongestüzten Risswachstum ferritischer Stähle in sauerstoffhaltigem Hochtemperaturwasser, Thesis, University of Stuttgart (1996) (a) section 7, (b) section 4

[6] D. Z. Sun, M. Sester, R. Mohrmann, R. Westerheide, H. Riedel, and H Yuan, H. P. Seifert and J. Heldt, Berechnung des Spannungs- und Deformationszustandes in der Umgebung eines Risses unter Korrosiven Bedingungen, Report V 158/98 of Fraunhofer Institut Werkstoffmechanik, Freiburg (D) and Paul Scherrer Institut, Villigen (CH), (1998)

[7] P.L. Andresen and L. M. Young, Characterization of the Roles of Electrochemistry, Convection and Crack Chemistry in Stress Corrosion Cracking, Proc. Seventh Int. Symposium on Environmental Degradation of Materials in Nuclear Power Systems - Water Reactors, NACE, (1995), 579,596

[8] D. Landolt, Corrosion et Chimie de Surfaces des Métaux, Presses Polytechniques et Universitaires Romandes (1993), sections 4, 5 and 7